MISSOURI
S&T

Missouri University of Science and Technology

Scholars' Mine

Physics Faculty Research & Creative Works

Physics

01 Feb 1974

Pb and Bi L-Subshell Ionization Cross-Section Ratios Versus Proton Bombarding Energy from 0.5 to 4 MeV

Don H. Madison
Missouri University of Science and Technology, madison@mst.edu

A. B. Baskin

C. E. Busch

Stephen M. Shafroth

Follow this and additional works at: https://scholarsmine.mst.edu/phys_facwork

Part of the Physics Commons

Recommended Citation

Pb and Bi L-subshell ionization cross-section ratios versus proton bombarding energy from 0.5 to 4 MeV[†]

D. H. Madison*

University of North Carolina, Chapel Hill, North Carolina 27514

A. B. Baskin, C. E. Busch,[‡] and S. M. Shafroth

University of North Carolina, Chapel Hill, North Carolina 27514

Triangle Universities Nuclear Laboratory, Durham, North Carolina 27706

(Received 2 July 1973)

Experimental ratios of L-subshell cross sections are given for ionization of lead and bismuth by 0.5-4-MeV-proton bombardment. The ratio of the L_{II} to L_I cross sections exhibits a maximum near 1.75 MeV. Individual subshell cross sections are obtained from the experimental ratios and previous total-cross-section data. These subshell ratios and cross sections are compared with the theoretical predictions of the plane-wave Born approximation using nonrelativistic hydrogenic wave functions, of the binary-encounter approximation scaled from Mg K-shell cross sections, and of the binary-encounter approximation scaled from cross sections obtained using L-shell velocity distributions. It was found that both approximations predict the trend of the data for the L_{II} and L_{III} subshells, but that only the plane-wave Born approximation gave the proper behavior for the L_I subshell.

I. INTRODUCTION

The first measurement of L x-ray yields arising from heavy–charged-particle bombardment was done by Bernstein and Lewis[1] who used scintillation counters to detect the x rays. The development of this type of work has been summarized by Merzbacher and Lewis.[2]

The advent of cooled semiconductor x-ray detectors with much better resolution has provided the means for a more detailed comparison between experimental and theoretical cross sections. Previously, total L x-ray cross sections and ratios of certain components comprising the L peak as a function of bombarding energy for heavy targets such as Au,[3] Pb,[4] Bi, and U[5] have been studied. Comparisons between experiment and the theoretical predictions of the plane-wave Born-approximation (PWBA) calculations and binary-encounter-approximation (BEA) calculations have been encouraging in certain cases. During the course of this work, better resolution Si(Li) detectors became available. The improved resolution has made a direct comparison of experimental and theoretical L-subshell cross sections feasible. In this work, we report such a comparison for the ionization of Pb and Bi by protons. We have assumed here that the probability for multiple ionization is small. The present work has been the subject of a previous communication.[6] Similar work on subshell cross sections has done for Au.[7]

II. EXPERIMENT

The experimental configuration was similar to that which has been reported previously.[3,4] The Triangle Universities Nuclear Laboratory (TUNL) 4-MeV Van de Graaff accelerator was used to produce nA beams of protons. Proton energies between 0.5 and 4.0 MeV were used to bombard thin Pb and Bi targets. The targets were prepared by evaporation onto a thin carbon foil which was used for support. The target thickness was chosen to minimize proton energy loss and self-absorption in the target. The thickness of the targets was determined and monitored during the data acquisition using Rutherford scattering at 90° for low-energy protons. The lead target was 35 $\mu g/cm^2$ and the bismuth target was 100 $\mu g/cm^2$.

The characteristic L x rays were detected using a KeVex Si(Li) detector with a resolution of 190 eV at 8 keV. The x rays passed through a 0.001-in Mylar window, a 0.5-in air path and a 0.001-in Be window before being detected. The targets were sufficiently thin and the air path was sufficiently short so that the absorption correction canceled when ratios of principle lines were taken.

Pulse-height spectra were acquired using a DDP224 on-line computer. Generally, data were acquired until the height of the strongest $L\gamma$ component was 1000 counts or more. Figure 1 shows a typical spectrum for bismuth at 3.0-MeV proton energy.

Decompositions of composite peaks as well as the determination of the intensities of single lines were made using an interactive data analysis program capable of fitting up to four Gaussians in a region of interest. The decomposition of multiple lines was performed using an iterative least-square-fitting algorithm due to Bevington.[8] The algorithm fits a function of the form of a straight-
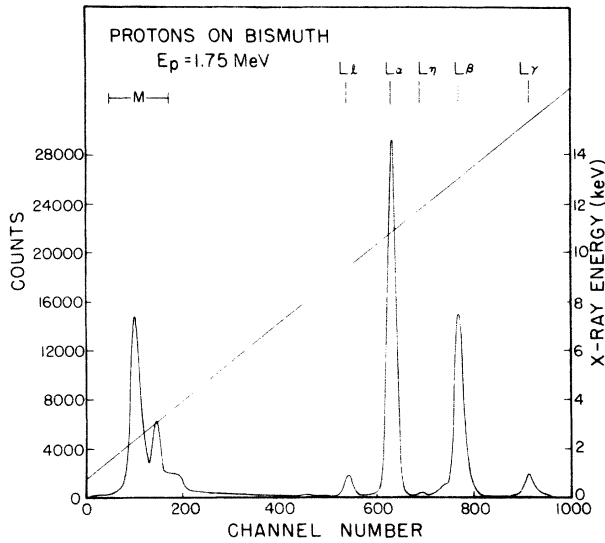
FIG. 1. Typical pulse-height spectrum for Bi.

line background plus from one to four Gaussian error functions. The fit is in the least-squares sense in that iteration is terminated when a minimum in the sum of the squares of the deviations of the fitted points is found. To minimize the effect of the choice of starting conditions, the amplifier gains for each element were held constant for all proton energies and the same starting parameters (except for appropriate adjustments of amplitudes) were used for all fits.

The Ll, $L\alpha$, $L\eta$ lines were fitted using a single Gaussian. The composite nature of the $L\alpha$ peak caused a slight broadening in this line. The $L\beta$ peak was fitted with three Gaussians. However, the lowest- and highest-energy components of $L\beta$ constituted such a small a fraction of the total $L\beta$
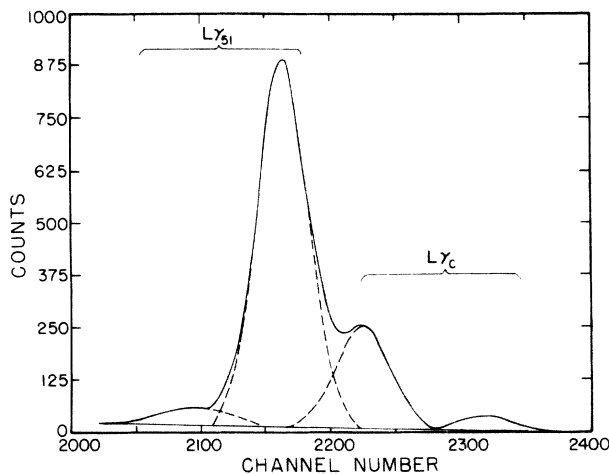

FIG. 2. Decomposition of the $L\gamma$ peak of Pb taken at $E_p = 3.0$ MeV.

that it was not statistically feasible to use them separately. The $L\gamma$ line was decomposed into four Gaussians and the constituents of each were identified. Figure 2 shows a typical decomposition of the lead $L\gamma$ structure for a proton energy of 3.0 MeV. For the purposes of this work the areas of the two lowest-energy peaks (involving only transitions to the L_{II} subshell) have been combined and labeled $L\gamma_{51}$, while the two higher-energy peaks have have been combined and labeled $L\gamma_c$. Experimental ratios of peak areas are given in Table I.

It was found that the $L\alpha/L\beta$ data presented in Table II of Ref. 4 differed by 4–13% from the present data for lead where the bombarding energies overlapped. The source of this difference may have been related to the masks used in Ref. 4. The data of Table I of the present paper are thought to be more reliable than the data in Table II of Ref. 4. The errors quoted for the total cross sections presented in Table I of Ref. 4 are large enough to account for most of the additional uncertainty caused by this difference in the ratios.

III. DETERMINATION OF SUBSHELL CROSS-SECTION RATIOS

Using the procedure described above, we were able to extract the $L\alpha$, $L\beta$, $L\gamma_{51}$, and $L\gamma_c$ peak areas with good statistical accuracy. The energies of the transitions in these peaks, their radiative widths as calculated by Scofield,[9] and subshell of

TABLE I. Experimental ratios used in determining L-sub- shell cross-section ratios.

| Proton energy (MeV)	$I_{L\alpha}/I_{L\beta}$	$I_{L\alpha}/I_{L\gamma_{51}}$	$I_{L\alpha}/I_{L\gamma_c}$
	Lead		
0.5	1.86 ± 0.11	23.4 ± 1.4	30.8 ± 2.2
0.75	1.90 ± 0.05	19.5 ± 0.8	46.9 ± 1.9
1.0	1.86 ± 0.03	16.9 ± 0.5	62.1 ± 2.6
1.5	1.80 ± 0.02	15.4 ± 0.4	75.0 ± 2.8
1.75	1.75 ± 0.02	14.1 ± 0.5	76.2 ± 3.7
2.0	1.72 ± 0.01	14.1 ± 0.2	71.3 ± 1.6
2.5	1.66 ± 0.01	13.7 ± 0.2	58.0 ± 1.6
2.75	1.63 ± 0.03	13.3 ± 0.2	54.6 ± 1.7
3.0	1.61 ± 0.01	13.2 ± 0.3	47.9 ± 1.2
	Bismuth		
0.5	1.86 ± 0.07	21.6 ± 1.0	29.3 ± 1.1
0.75	1.92 ± 0.11	19.2 ± 0.5	41.0 ± 1.1
1.0	1.94 ± 0.03	17.6 ± 0.5	54.5 ± 1.8
1.25	1.91 ± 0.02	16.3 ± 0.3	69.3 ± 2.6
1.5	1.89 ± 0.03	14.9 ± 0.8	71.7 ± 2.7
1.75	1.83 ± 0.02	14.5 ± 0.3	71.2 ± 2.1
2.0	1.78 ± 0.02	14.0 ± 0.3	67.6 ± 2.2
2.5	1.74 ± 0.02	13.5 ± 0.3	55.7 ± 1.7
3.0	1.70 ± 0.03	13.3 ± 0.3	47.7 ± 1.5
3.5	1.65 ± 0.05	13.1 ± 0.3	41.4 ± 1.0
4.0	1.63 ± 0.07	12.8 ± 0.5	40.9 ± 1.7
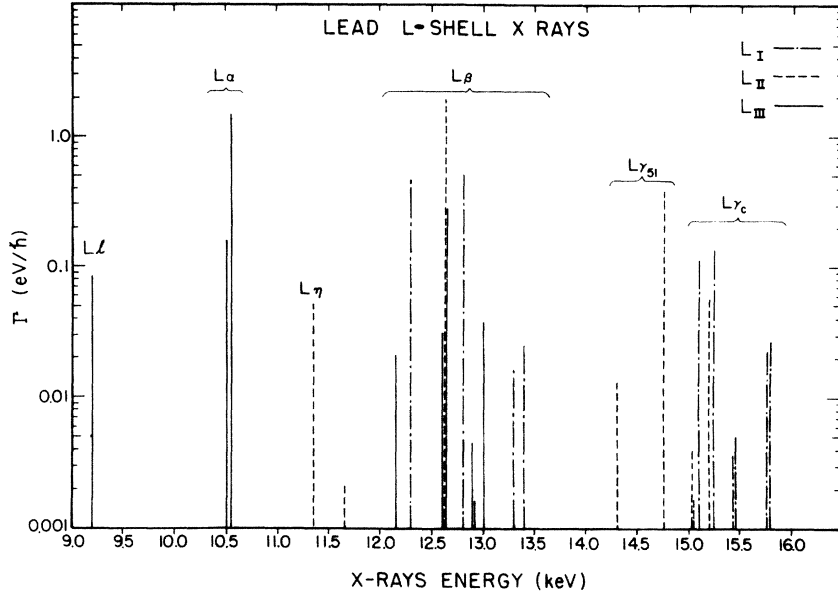
FIG. 3. Radiative widths according to Scofield's calculations (see Ref. 9). Energies for the transitions are taken from Bearden's tables (see Ref. 25). Subshell holes of origin are as indicated.

origin are shown in Fig. 3. The intensities of these peaks can be expressed in terms of the subshell cross sections σ_i, the fluorescence yields ω_i, and the Coster-Kronig transition probabilities f_{ij} as follows[3,10]:

$$I_{L\alpha} = K[(f_{13} + f_{12}f_{23})\sigma_1 + f_{23}\sigma_2 + \sigma_3]\omega_3 F_{3\alpha}, \quad (1)$$

$$I_{L\beta} = K\{[(f_{13} + f_{12}f_{23})\sigma_1 + f_{23}\sigma_2 + \sigma_3]\omega_3 F_{3\beta}$$

$$+ (f_{12}\sigma_1 + \sigma_2)\omega_2 F_{2\beta} + \sigma_1\omega_1 F_{1\beta}\}, \quad (2)$$

$$I_{L\gamma_{51}} = K(f_{12}\sigma_1 + \sigma_2)\omega_2 F_{2\gamma_{51}}, \quad (3)$$

$$I_{L\gamma_c} = K[(f_{12}\sigma_1 + \sigma_2)\omega_2 F_{2\gamma_c} + \sigma_1\omega_1 F_{1\gamma_c}], \quad (4)$$

where K is a constant whose value depends on target thickness, number of incident protons, solid angle, detector efficiency, and absorption. The quantity $F_{i\phi}$ is the fraction of the radiative transitions to the ith subshell associated with the $L\phi$ peak. An examination of the above relationships reveals that the four equations are not linearly independent. Expressing $L\beta$ in terms of the other three lines we get

$$I_{L\beta} = \frac{F_{3\beta}}{F_{3\alpha}} I_{L\alpha} + \frac{F_{1\beta}}{F_{1\gamma_c}} I_{L\gamma_c} + \left(\frac{F_{2\beta}}{F_{2\gamma_{51}}} - \frac{F_{1\beta}}{F_{1\gamma_c}}\frac{F_{2\gamma_c}}{F_{2\gamma_{51}}}\right) I_{L\gamma_{51}}. \quad (5)$$

Since most of the systematic errors involved in the experiment can be eliminated by working with ratios of peak intensities, we can express (5) as

$$\frac{I_{L\beta}}{I_{L\alpha}} = A + B\frac{I_{L\gamma_c}}{I_{L\alpha}} + C\frac{I_{L\gamma_{51}}}{I_{L\alpha}}, \quad (6)$$

where A, B, and C are assigned the obvious values

and are functions of the $F_{i\phi}$'s. Assuming that the $F_{i\phi}$'s are independent of energy, the data at various energies may be used to find experimental values for A, B, and C. Theoretical values for these quantities may be obtained from the calculations of Scofield[9] or Rosner and Bhalla[11] (for a review of calculations of this type, see Ref. 12). Salem and Schultz[13] have obtained experimental L x-ray transition probabilities by forming a least-squares fit to available experimental data. This work does not include all the lines that can contribute to a

TABLE II. Ratios of relative x-ray emission rates.

	Expt.	Scofield[a]	Salem and Schultz[b]
		Lead	
$\dfrac{F_{3\beta}}{F_{3\alpha}}$	0.252 ± 0.026	0.219	0.270
$\dfrac{F_{1\beta}}{F_{1\gamma_c}}$	3.29 ± 0.66	3.18	4.48
C^c	3.99 ± 0.37	4.31	4.04
		Bismuth	
$\dfrac{F_{3\beta}}{F_{3\alpha}}$	0.262 ± 0.033	0.234	0.277
$\dfrac{F_{1\beta}}{F_{1\gamma_c}}$	3.18 ± 0.77	3.15	4.43
C^c	3.48 ± 0.42	4.26	3.98

[a] See Ref. 9. The calculation described by Rosner and Bhalla (Ref. 11) gives results very similar to these.

[b] See Ref. 13.

[c] $C = \dfrac{F_{2\beta}}{F_{2\gamma_{51}}} - \dfrac{F_{1\beta}}{F_{1\gamma_c}}\dfrac{F_{2\gamma_c}}{F_{2\gamma_{51}}}$.

TABLE III. Relative x-ray emission rates.

	$F_{1\beta}$	$F_{1\gamma_c}$	$F_{2\beta}$	$F_{2\gamma_{51}}$	$F_{3\beta}$	$F_{3\alpha}$
			Lead			
Expt.	0.742	0.225	0.779	0.178	0.193	0.766
Scofield	0.735	0.232	0.789	0.168	0.172	0.787
			Bismuth			
Expt.	0.736	0.231	0.758	0.197	0.203	0.773
Scofield	0.734	0.233	0.787	0.168	0.185	0.791

given peak, but it can be used to give an estimate for A, B, and C from previous experimental work. In Table II, we show the values of A, B, and C that have been determined from our data for Pb and Bi using a least-squares method, the theoretical values calculated by Scofield,[9] and previous experimental values obtained from the tabulation of Salem and Schultz.[13] The theoretical calculations of Rosner and Bhalla[11] are not shown since they are very similar[11,12] to those of Scofield. Examination of Table II reveals that the theoretical results generally lie within our experimental error. It is interesting to note that if one uses Scofield's results to estimate the contributions of the lines not tabulated by Salem and Schultz, the resulting change improves agreement between our results and the least-squares fit to previous experimental
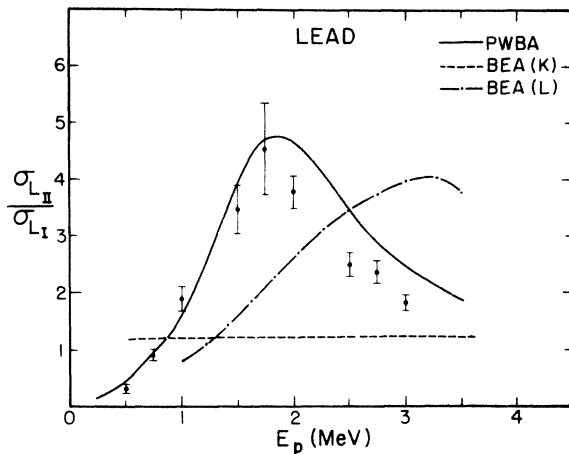
work. The value of the branching ratio $F_{1\beta}/F_{1\gamma_c}$ for Pb is in reasonable accord with the value of 2.83 ± 0.43 given by Rao et al.[14]

The experimental ratios A, B, and C can be used to find experimental values for the $F_{i\phi}$'s. The sum of $F_{i\phi}$ over all lines $L\phi$ that contribute to a given subshell i must be unity. Therefore, if the spectra which we are considering included all possible lines contributing to each subshell, we could set the sum of our F's for each subshell equal to 1. However, there are some weak lines which are not included in the spectra reported here. This means that the sum of the present F's for a given subshell will be less than unity. According to the calculation of Scofield, the lines not considered here would make contributions to this sum on the order of 0.02–0.05 for these subshells of Pb and Bi. It has been previously noted that Scofield's calculation generally lies within the experimental error of 10–20%. We therefore use Scofield's results for the lines not included in this work. It is to be noted that an error of as much as 50% in the Scofield number would change the sum which we use by only 1–2%. Then, within this framework,

$$F_{1\beta} + F_{1\gamma_c} = S_1, \tag{7}$$

$$F_{2\beta} + F_{2\gamma_{51}} = S_2, \tag{8}$$

and

$$F_{3\beta} + F_{3\alpha} = S_3, \tag{9}$$

where S_i ranges from 0.95 to 0.98 for Pb and Bi. Note that $F_{2\gamma_c}$ is not included in (8). This was omitted since it is on the order of 0.02 and cannot be determined from our data. Using the above with Scofield's values for the weak lines and the experimental values for A, B, and C, experimental $F_{i\phi}$'s can be found. These are presented in Table III.

Subshell cross-section ratios can now be found

FIG. 4. Ratio of L_{II}- to L_I- subshell cross sections for Pb as a function of proton energy. The experimental errors reflect only the statistical uncertainties in the peak areas and do not inlcude uncertainties in the $F_{i\phi}$'s, Coster-Kronig yields, or fluorescence yields. The theoretical curves are solid curve: PWBA cross sections of Choi et al.; broken curve: BEA scaled from Mg K-shell cross sections of Garcia; dash-dot curve: BEA scaled from L-shell cross sections calculated by Hansen.
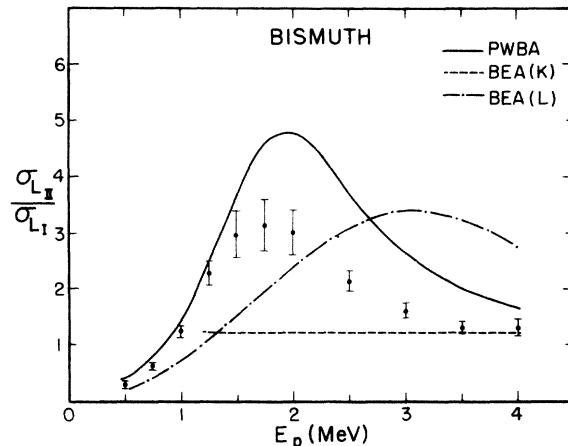

FIG. 5. Same as Fig. 4 except here the target is Bi.

from the three linearly-independent equations (1), (3), and (4) assuming the fluorescence yields and Coster-Kronig probabilities are known. From these equations it is readily seen that

$$\frac{\sigma_2}{\sigma_1} = \frac{\omega_1}{\omega_2}\left(\frac{F_{2\gamma_{51}}}{F_{1\gamma_c}}\frac{I_{L\gamma_c}}{I_{L\gamma_{51}}} - \frac{F_{2\gamma_c}}{F_{1\gamma_c}}\right)^{-1} - f_{12},\qquad(10)$$

and

$$\frac{\sigma_3}{\sigma_2} = \frac{\omega_2}{\omega_3}\frac{F_{2\gamma_{51}}}{F_{3\alpha}}\frac{I_{L\alpha}}{I_{L\gamma_{51}}}$$

$$\times\left(1+f_{12}\frac{\sigma_1}{\sigma_2}\right) - (f_{13}+f_{12}f_{23})\frac{\sigma_1}{\sigma_2} - f_{23}.\qquad(11)$$

IV. RESULTS AND CONCLUSIONS

Experimental results for σ_2/σ_1 as a function of proton energy are shown in Figs. 4 and 5 for lead and bismuth, respectively. For lead, the experimental fluorescence yields and Coster-Kronig probabilities of Rao et al.[14,15] and Wood et al.[16] were used in determining the subshell cross-section ratios. For bismuth, the experimental values of Fink and Freund[17,18] were used. The error bars in the figures represent statistical uncertainties and do not include uncertainties in the $F_{i\phi}$'s, fluorescence yields, or Coster-Kronig probabilities. Also shown in Figs. 4 and 5 are the theoretical results of the PWBA obtained from nonrelativistic hydrogenic wave functions,[19] of the BEA scaled from Mg K-shell cross sections of Garcia,[20] and of the BEA scaled from L-subshell cross sections (Ref. 21, Table I) calculated by Hansen. (These

L-subshell cross sections were obtained using L-subshell momentum-space velocity distributions.) Similar results for σ_3/σ_2 are shown in Figs. 6 and 7.

It is seen from Figs. 4 and 5 that the data for σ_2/σ_1 have a maximum near 1.75 MeV that is predicted by the PWBA. The BEA scaled from L-shell cross sections does predict a peak in this ratio but at a considerably higher energy, while the BEA scaled from Mg K-shell cross sections does not predict a peak. It is to be expected that the latter BEA would not predict this maximum since it results from a node in the 2s wave function.[22] A variety of different experimental quantities have been used in obtaining these experimental cross sections. Varying the quantities not determined by the present data causes the experimental points to shift uniformly in the vertical direction. Since the proton energy at which the maximum in the σ_2/σ_1 ratio occurs is unaffected by such a shift, it is significant that the PWBA predicts the proper energy for the maximum while the BEA does not.

It is seen from Figs. 6 and 7 that there is also good agreement between the experimental data and the PWBA for the subshell cross-section ratio σ_3/σ_2. The BEA ratios obtained from the L-shell cross sections are not shown here since the interpolation required to find cross sections at the same energy was not sufficiently reliable. The values were generally similar to those shown for the BEA scaled from Mg however. The differences between the PWBA and the BEA scaled from Mg are not as pronounced for the σ_3/σ_2 ratio as they were for σ_2/σ_1. This probability originates from the similarity between the 1s and 2p wave functions.

The least-certain experimental quantities used in obtaining the subshell cross-section ratios are
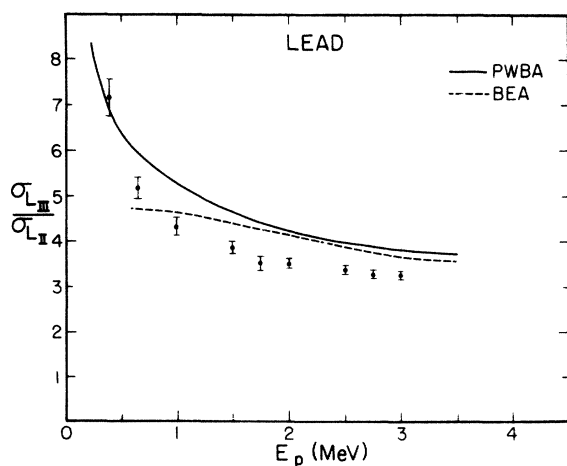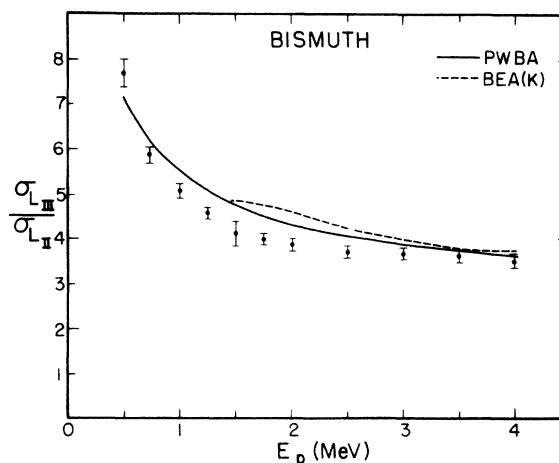

FIG. 6. Ratio of L_{III} - to L_{II}-subshell cross sections for Pb as a function of proton energy. The experimental errors reflect only statistical uncertainties in the peak areas. The theoretical curves are solid curve: PWBA cross sections of Choi et al.; broken curve: BEA scaled from Mg K-shell cross sections of Garcia.

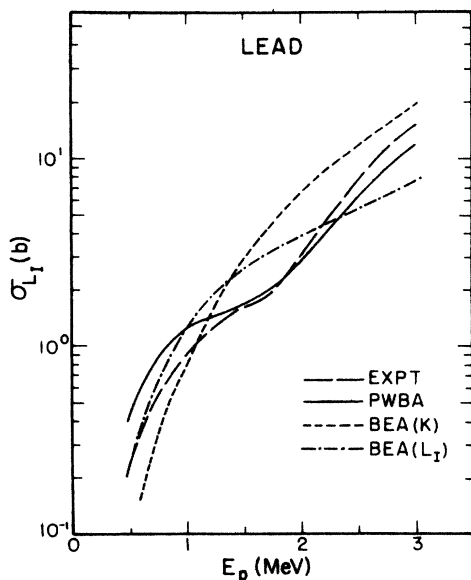FIG. 7. Same as Fig. 6 except here the target is Bi.

FIG. 8. Cross sections for ionization of the L_I sub-
shell of Pb. The PWBA cross sections are those of Choi
et al. The BEA cross sections were obtained by scaling
from the Mg K-shell cross sections of Garcia and scaling
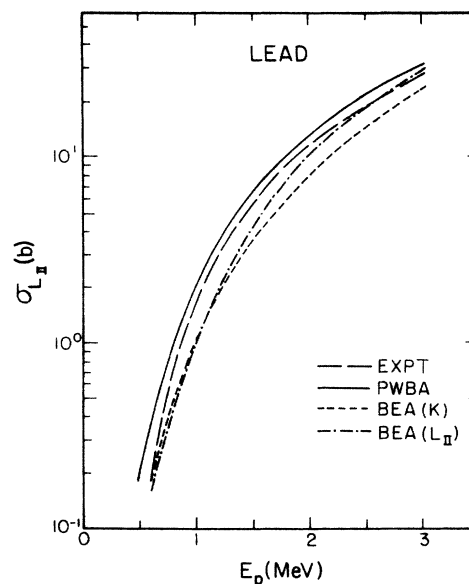from the L-shell cross sections calculated by Hansen.

the Coster-Kronig probabilities. This does not
present a severe problem, however, since the
Coster-Kronig probabilities do not greatly affect
the results. For example, the first term of Eq.
(10) represents approximately 90–96% of the final
results and the first term of (11) represents
90–98% of the final results. With this fact in mind,
it is seen from (10) and (11) that the subshell
cross sections depend strongly on the fluorescence
yields. For example, if we had used the experi-
mental fluorescence yields for bismuth of Ross
et al.[23] instead of those of Fink and Freund, the
data for σ_2/σ_1 would lie above the Born curve in-
stead of below it.

Individual subshell cross sections may be ob-
tained from the subshell ratios and the total
L-shell cross section. The total L-shell cross
section for Pb may be acquired from the total
L-shell x-ray cross section of Busch *et al.*[4] and
the average L-shell fluorescence yield of Patronis
et al.[24] Figures 8 and 9 show the trend of the ex-
perimental data for the L_I and L_{II} subshell cross
sections for Pb. Variations in the average fluo-
rescence yield can shift the data uniformly in the
vertical direction. Also shown are the theoretical

FIG. 9. Same as Fig. 8 except for ionization of the
L_{II} subshell.

predictions of the PWBA using nonrelativistic
hydrogenic wave functions,[19] of the BEA scaled
from Mg K-shell cross sections,[20] and of the BEA
scaled from L-shell cross sections.[21] From Fig.
8, it is seen that the trend of the data for σ_1 is
predicted by the PWBA calculation but not the BEA
calculations. However, all the calculations predict
the general trend of the data for σ_2. Results for
σ_3 (not shown) are very similar to those for σ_2. It
is interesting to note that the BEA curve scaled
from K-shell cross sections predicts the shape of
the data better than the BEA curve scaled from
L-shell cross sections.

In summary, a maximum in the ratio σ_2/σ_1 for
Pb and Bi has been found near 1.75 MeV. The
PWBA calculation exhibited a maximum at the
proper proton energy, but the BEA calculations
did not. This failure of the BEA calculations was
seen to originate primarily from improper predic-
tion of the σ_1 cross section. Both the PWBA and
the BEA gave the trend of the data for σ_2 and σ_3.

[1] E. M. Bernstein and H. W. Lewis, Phys. Rev. 95, 83 (1954).

[2] E. Merzbacher and H. W. Lewis, *Encyclopedia of Physics* (Springer-Verlag, Berlin, 1958), Vol. 34, p. 166.

[3] S. M. Shafroth, G. A. Bissinger, and A. W. Waltner, Phys. Rev. A 7, 566 (1973). See also G. A. Bissinger, A. B. Baskin, B.-H. Choi, S. M. Shafroth, J. M. Howard, and A. W. Waltner, Phys. Rev. A 6, 545 (1972).

[4] C. E. Busch, A. B. Baskin, P. H. Nettles, S. M. Shafroth, and A. W. Waltner, Phys. Rev. A 7, 1601 (1973).

[5] J. T. May, A. W. Waltner, A. B. Baskin, C. E. Busch, and S. M. Shafroth, Bull. Am. Phys. Soc. 18, 83 (1973); C. E. Busch, A. B. Baskin, B. Doyle, S. M. Shafroth, and A. W. Waltner, Bull. Am. Phys. Soc. 18, 83 (1973).

[6] A. B. Baskin, C. E. Busch, D. H. Madison, and S. M. Shafroth, Bull. Am. Phys. Soc. 18, 83 (1973).

[7] E. Laegsgaard and S. Datz (private communication, 1973).

[8] P. Bevington, *Data Reduction and Error Analysis for Physical Science* (McGraw-Hill, New York, 1969).

[9] J. H. Scofield, Phys. Rev. 179, 9 (1969).

[10] W. Bambynek, B. Crasemann, R. W. Fink, H. -U. Freund, H. Mark, C. D. Swift, R. E. Price, and P. V.

Rao, Rev. Mod. Phys. 44, 716 (1972).

[11] H. R. Rosner and C. P. Bhalla, Z. Phys. 231, 347 (1970).

[12] S. I. Salem, in *Proceedings of the International Conference on Inner-Shell Ionization Phenomena and Future Applications,* edited by R. W. Fink, S. T. Manson, J. M. Palms, and P. Venugopala Rao (U. S. AEC, Oak Ridge, Tenn., 1972), pp. 285–316.

[13] S. I. Salem and C. W. Schultz, At. Data 3, 215 (1971).

[14] P. Venugopala Rao, J. M. Palms, and R. E. Wood, Phys. Rev. A 3, 1568 (1971).

[15] P. Venugopala Rao, R. E. Wood, J. M. Palms, and R. W. Fink, Phys. Rev. 178, 1997 (1969).

[16] R. E. Wood, J. M. Palms, and P. Venugopala Rao, Phys. Rev. A 5, 11 (1972).

[17] R. W. Fink and H. -U. Freund, Phys. Rev. C 3, 1701 (1971).

[18] H.-U. Freund and R. W. Fink, Phys. Rev. 178, 1952 (1969).

[19] B.-H. Choi, E. Merzbacher, and G. S. Khandelwal, At. Data 5, 291 (1973).

[20] J. D. Garcia, Phys. Rev. A 1, 280 (1970).

[21] J. S. Hansen, Phys. Rev. A 8, 822 (1973).

[22] E. Merzbacher, in Ref. 12, pp. 915–935.

[23] M. A. S. Ross, A. J. Cochran, J. Hughes, and N. Feather, Proc. Phys. Soc. Lond. A 68, 612 (1955).

[24] E. T. Patronis, Jr., C. H. Braden, and L. D. Wyly, Phys. Rev. 105, 681 (1957).

[25] J. A. Bearden, Rev. Mod. Phys. 39, 78 (1967).